

LONGITUDINAL MEASUREMENTS AND BEAM TUNING IN THE J-PARC LINAC MEBT1

M. Otani*, K. Futatsukawa, T. Miyao, Y. Liu, KEK, Oho, Tsukuba, 305-0801, Japan
 K. Hirano, Y. Kondo, A. Miura, H. Oguri, JAEA, Tokai, Ibaraki, 319-1195, Japan

Abstract

The Japan Proton Accelerator Research Complex (J-PARC) linac is operated with design peak current of 50 mA from 2018. For operation with such a high beam current, it is important to understand transverse and longitudinal beam properties especially in low-velocity region. A medium energy beam transport (MEBT1) line between the 3-MeV radio-frequency quadrupole linac (RFQ) and the 50-MeV drift-tube linac (DTL) is a 3-m-long transport line to match the beam to the DTL and produces a macro pulse configuration for a 3-GeV rapid-cycling synchrotron (RCS). In this paper, recent measurements and beam tuning results in MEBT1 will be presented.

INTRODUCTION

The Japan Proton Accelerator Research Complex (J-PARC) linac consists of a 50-keV negative hydrogen (H^-) ion source (IS), a 3-MeV radio-frequency quadrupole linac (RFQ), a 50-MeV drift-tube linac (DTL), a 191-MeV separated-type DTL (SDTL), and a 400-MeV annular-ring coupled structure (ACS). A medium-energy beam transport section (MEBT1) is installed between the RFQ and DTL in order to produce a macro pulse configuration for a 3-GeV rapid-cycling synchrotron (RCS).

The J-PARC linac is operated with design peak current of 50 mA from 2018. Further, a higher beam current is being investigated for future projects at J-PARC. For operation with such a high beam current, it is important to understand transverse and longitudinal beam properties especially in MEBT1 because space charge effect is most prominent.

In this paper, the beam measurements and current status of the beam tuning at MEBT1 are presented. First, we show beamline components in MEBT1. Then, we show results of the beam measurements and beam tuning at MEBT1. Finally, we summarize our results.

BEAMLINER

MEBT1 is a 3-m-long transport line, as shown in Fig. 1. MEBT1 has two main functions. One is the matching of the beam to the DTL. Eight quadrupole magnets (Q1 to Q8) and two buncher cavities are used for this purpose. The other is the production of a macro pulse configuration in accordance with the radio-frequency of the RCS. The radio-frequency deflector (RFD) and a scraper located 0.72 m downstream from the RFD serve this function; unnecessary beam bunches are horizontally deflected by the RFD and then dumped to the scraper.

* masashio@post.kek.jp

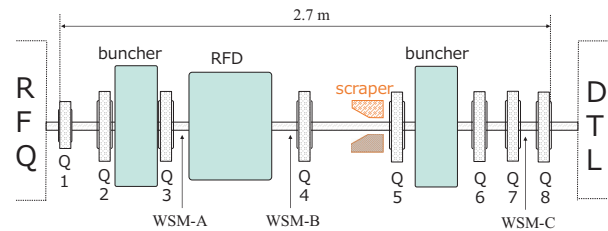


Figure 1: Schematic of MEBT1.

The RFD consists of two radio-frequency gaps operated in a TE_{11} -like mode. The operation frequency is 324 MHz which is same as that of the RFQ and DTL. The distance between the gaps corresponds to $3\beta\lambda$, where β is the particle velocity normalized to the speed of light and λ is a radio-frequency wavelength. Because the two radio-frequency gaps are independently operated with a semiconductor amplifier with a peak power of 120 kW [1], the synchronous phase and radio-frequency voltage are tuned individually. The design electric field for deflecting beam is 2.6 MV/m and deflecting angle is 6 mrad.

The transverse beam profiles are measured by a wire scanner monitor (WSM) [2]. The WSM employs $7\ \mu\text{m}$ diameter carbon wire. Because the frame is installed with 45° against the horizontal axis and the frame has two wires in the horizontal and vertical directions, the horizontal and vertical profiles can be measured. The head is moved by 0.1 mm step using a stepping motor unit. In this paper, three WSMs (WSM-A, WSM-B, and WSM-C shown in Fig. 1) were used.

MEASUREMENT AND TUNING

Transverse Measurement

The Courant–Snyder parameters in the transverse direction were measured by so-called Q-scan method. The beam profile in the horizontal and vertical directions were measured using the pair of Q3 and WSM-B and the pair of Q2 and WSM-A, respectively. The measurements were performed at different quadrupole field strength. Almost 100% beam transmission to the beam current monitor located behind the WSM is maintained during the measurements. In order to treat the transverse direction independently to the longitudinal direction, the buncher cavity was not operated during the measurements.

Figure 2 shows the transverse beam size measured by the WSMs. The measurements were performed at different period: October 2018 and March 2019. An RF antenna in the IS module was replaced as a regular maintenance work

Content from this work may be used under the terms of the CC BY 3.0 licence (© 2019). Any distribution of this work must maintain attribution to the author(s), title of the work, publisher, and DOI

This is a preprint — the final version is published with IOP

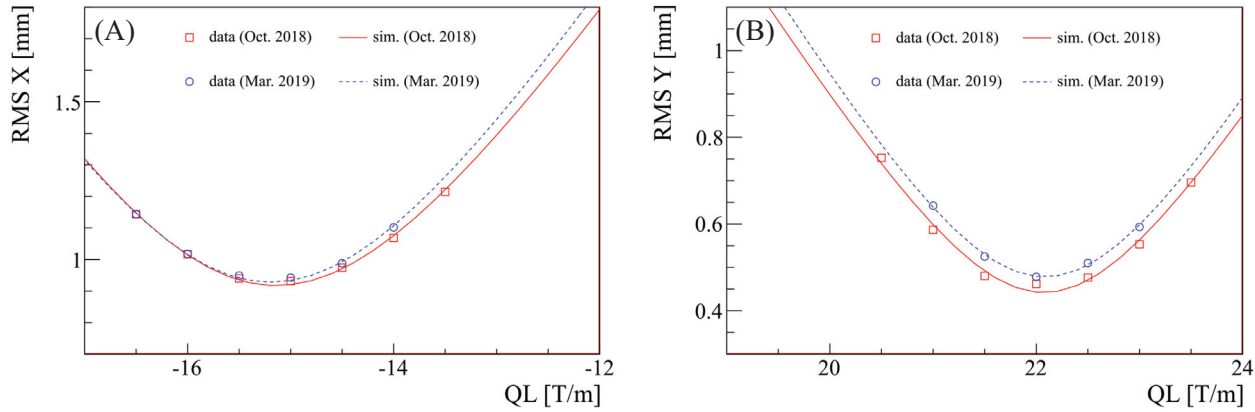


Figure 2: Transverse beam sizes in rms as a function of the quadrupole strength. (A) horizontal, (B) vertical. Two measurement results at different period (red square: Oct. 2018, blue circle: Mar. 2019) are shown along with the fitting by the PIC simulation (red line: Oct. 2018, blue dot line: Mar. 2019).

between each period and a beam transport line between IS and RFQ was optimized in each period.

To estimate the beam parameters, the beam dynamics simulations were performed using IMPACT, which is three-dimensional particle-in-cell code [3]. The Courant–Snyder parameters of the beam exiting the RFQ were fitted by employing the SIMPLEX algorithm [4]. The simulation results with the fitted beam parameters are shown by the smooth curves in Fig. 2. The measurements and the simulations are consistent within few percents.

Figure 3 shows designed and measured rms phase space ellipses. The fitted transverse emittance is 0.2π mm mrad, which is consistent with the LINACsrfq [5] simulation within several percents. The mismatch factor [6] between designed and measured ellipses is less than 0.2 in all the results. It corresponds to approximately 10% additional emittance growth due to the beam mismatch to DTL, which is acceptable for the stable operation. The difference of emittance between two periods is several percents. The cause of the difference is considered to be due to the different parameters of the upstream beam.

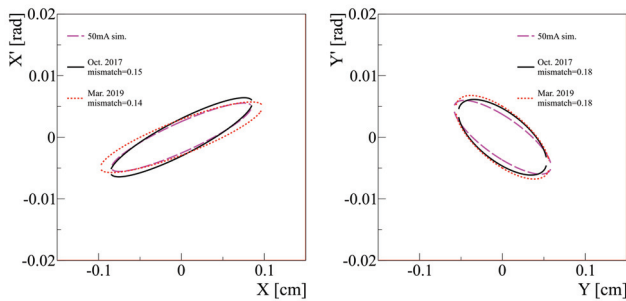


Figure 3: Designed (purple dashed) and measured rms phase space ellipses of the beam exiting the RFQ. Black line: Oct. 2018, red dot: Mar. 2019.

Longitudinal Measurement

The Courant–Snyder parameters in the longitudinal direction were measured using the RFD and WSMs [7]. In this measurement, the longitudinal bunch width is converted to the transverse one using the RFD. The transverse beam width is measured by the WSM downstream (WSM-B) and the longitudinal bunch width is reconstructed by comparing the beam width with and without the RFD operation. The longitudinal bunch width ($\langle \Delta\phi^2 \rangle$) is calculated from the beam width with the RFD operation ($\langle (x \pm k(\Delta\phi - \delta))^2 \rangle$) and without the RFD operation ($\langle x^2 \rangle$) as following equation:

$$\langle \Delta\phi^2 \rangle = \left[\frac{\langle (x + k(\Delta\phi - \delta))^2 \rangle / 2 + \langle (x - k(\Delta\phi - \delta))^2 \rangle / 2 - \langle x^2 \rangle}{k^2 + \delta^2} \right] \quad (1)$$

where x is the horizontal position, k represents the deflecting angle, and δ is the phase offset to the zero-crossing of the RF field in RFD.

Figure 4 shows the measured longitudinal bunch size as a function of the buncher radio-frequency voltages. In Fig. 4, measurement at two period is shown as blue square (Oct. 2019) and black circle (Nov. 2019). The upstream beam conditions are same during these periods. The measurements are consistent each other within the measurement error of 0.5 degrees.

The beam dynamics simulation is performed using IMPACT and the Courant–Snyder parameters of the beam exiting the RFQ were fitted with the SIMPLEX algorithm [4]. The error matrix was evaluated after fitting using the HESSE algorithm [8]. The simulation results with the fitted beam parameters are shown by the smooth curves in Fig. 4. The measured emittance is $0.15 \pm 0.01 \pi$ deg-MeV, which was consistent with the simulation result.

Tuning

Based on the measured phase space ellipses of the beam exiting the RFQ, the beam optics in MEBT1 is being optimized. As a first step, the beam envelope in the MEBT1

Content from this work may be used under the terms of the CC BY 3.0 licence (© 2019). Any distribution of this work must maintain attribution to the author(s), title of the work, publisher, and DOI

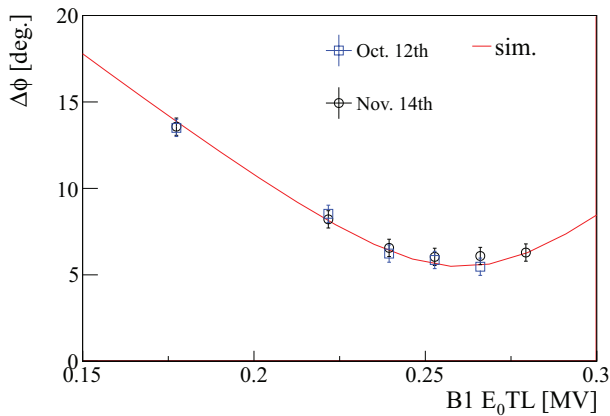


Figure 4: Result of the longitudinal bunch size measurements using the second gap of the RFD. The blue square and black circle show the measurement results on Oct. 2019 and Nov. 2019, respectively. The red line shows the fitting result by the IMPACT code.

was simulated by the IMPACT code and compared to the measurement by the WSMs. Figure 5 shows the result. Simulation and measurement are consistent at each location within approximately 0.1 mm. The rms drop-off in the horizontal direction at $z = 1.9$ m is due to loss at the scraper. The transmission at the scraper is also well reproduced by the simulation. We are developing the algorithm for designing the MEBT1 optics based on the results.

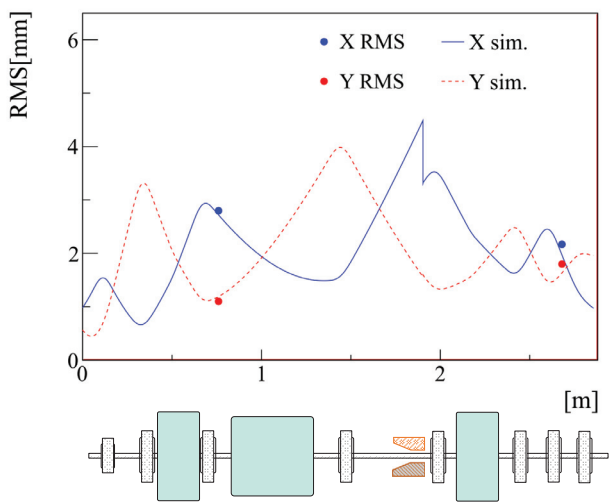


Figure 5: Beam envelope in the horizontal direction (blue line) and vertical direction (red dotted line) simulated by the IMPACT code along the measurements by the WSMs.

CONCLUSION

The J-PARC linac is providing design peak current of 50 mA from 2018 and aims a higher beam current for fu-

ture projects. The MEBT1 is most important to realize the higher beam current because the space charge effect is most prominent. We succeeded in measuring the transverse and longitudinal beam quantities at MEBT1 and reproducing the beam envelope in entire MEBT1 section. The design algorithm for the MEBT1 beam optics is being developed for better transmission at the scraper and further improvement of beam matching to downstream accelerator of DTL.

REFERENCES

- [1] K. Futatsukawa *et al.*, “Chopper Operation for the Tandem Scrapers at the J-PARC Linac”, in *Proc. 27th Linear Accelerator Conf. (LINAC’14)*, Geneva, Switzerland, Aug.-Sep. 2014, paper TUPP067, pp. 581–583.
- [2] A. Miura *et al.*, “Operational Performance of Wire Scanner Monitor in J-PARC Linac”, in *Proc. of the 1st International Particle Accelerator Conference (IPAC’10)*, Kyoto, Japan, May 2010, paper MOPE021, pp. 1008-1010.
- [3] J. Qiang *et al.*, “An object-oriented parallel particle-in-cell Code for beam dynamics simulation in linear accelerators.” *J. Comput. Phys.* vol. 163, pp. 434-451, 2000.
- [4] F. James and M. Roos, “Minuit: A System for Function Minimization and Analysis of the Parameter Errors and Correlations,” *Comput. Phys. Commun.*, vol. 10, pp. 343–367, 1975.
- [5] R.A. Jameson, “Equipartitioning in linear accelerators”, Oak Ridge National Laboratory, Oak Ridge, TN, USA, Rep. ORNL/TM-2007/001, 2007.
- [6] K.R. Crandall and D.P. Rustoi, “TRACE 3D Documentation”, Los Alamos National Laboratory, Los Alamos, New Mexico, USA, Rep. LA-UR-97-886, 1997.
- [7] M. Otani, K. Futatsukawa, K. Hirano, Y. Kondo, A. Miura, H. Oguri, Y. Liu, *Nucl. Instr. and Meth. in Phys. Res. Sec. A*, vol. 908, pp. 313-317, Nov. 11, 2018.
- [8] W.T. Eadie *et al.*, “Statistical Methods in Experimental Physics”. Amsterdam, The Netherlands: North-Holland, 1971.